Available online at www.sciencedirect.com

ScienceDirect

Journal of the European Ceramic Society 27 (2007) 3295–3299

www.elsevier.com/locate/jeurceramsoc

Anomalous high activation energy for creep in nanostructured 3YTZP/Ni cermets

A. Morales-Rodríguez[a], D. Gómez-García[a],
T. Rodriguez-Suarez[b], S. Lopez-Esteban[b],
C. Pecharroman[b], J.S. Moya[b], A. Domínguez-Rodríguez[a,*]

[a] *Departamento de Física de la Materia Condensada, Universidad de Sevilla, Apartado 1065, 41080 Sevilla, Spain*
[b] *Instituto de Ciencia de Materiales de Madrid, CSIC, Cantoblanco, 28049 Madrid, Spain*

Abstract

The plastic behavior of cermets based on a 3 mol% yttria-stabilized tetragonal zirconia matrix that incorporates nanometric nickel inclusions (3YTZP/n-Ni), with 2.5, 5 and 10 vol.% of nickel content, has been studied by constant load tests in compression carried out in argon atmosphere. The microstructure of these composites consists of nanometric nickel inclusions homogeneously dispersed into a fine-grained zirconia matrix (about 200 nm). The microstructural and mechanical results obtained show that the creep behavior is controlled by the zirconia matrix as in 3YTZP-based cermets with micrometric Ni inclusions (3YTZP/μ-Ni); whereas the stress exponent values are similar to those of high-purity monolithic 3YTZPs, anomalous high values of the activation energy have been measured. The ceramic/metal interface plays a crucial role for creep properties; the strong TZP/n-Ni interface matching can be at the origin of these high values of the activation energies for creep.

Keywords: Interfaces; Creep; Diffusion; ZrO_2; Cermet

1. Introduction

3YTZP/Ni cermets are metallic-ceramic materials comprising of nickel inclusions in a TZP matrix that are proposed for high-value added functional applications related to spatial industry, sensors applications and future energy sources.[1] These applications require to work at high temperatures so it is of importance to know their mechanical response in operating conditions. Nevertheless, the mechanical characteristics of 3YTZP/μ-Ni composites are not very appropriate due to the weak bonding between both 3YTZP and nickel phases.[2] The addition of micrometric nickel particles to 3YTZP embrittles the composites, decreasing the mechanical properties at room temperature[3] and no relevant effects on high-temperature behavior have been reported. Available studies conclude that creep is exclusively controlled by the zirconia matrix.[4,5]

Recently, Esteban-Betegon et al.[6] have prepared 3YTZP/n-Ni nanocrystalline composites by precipitation, reduction and sinterization of nickel salts on zirconia powder. These composites that have small amounts of nickel exhibit strong metal–ceramic bonds[7,8] and a remarkable hardening effect.[9]

This work has been focused on the influence of the metal–ceramic bonding on the plastic behavior of nanocrystalline zirconia–nickel composites. Three samples with different nickel content have been studied by means of creep tests conducted in argon atmosphere. The mechanical and microstructural results have been compared to the behavior of 3YTZP/μ-Ni microcomposites.[5]

2. Experimental procedure

2.1. Processing

2.1.1. Starting materials

The following commercial powders were used: (i) nickel(II) nitrate hexahydrate (Merck, Germany, 99.0% purity, $Ni(NO_3)_2{\cdot}6H_2O$) and (ii) tetragonal zirconia polycrystals (3YTZP; 3 mol% Y_2O_3; TZ-3YS, Tosoh Corp.), with an average particle size of $d_{50} = 0.26 \pm 0.05$ μm and a BET specific surface area of 6.7 m^2/g.

---

[*] Corresponding author. Tel.: +34 954557849; fax: +34 954612097.
E-mail address: adorod@us.es (A. Domínguez-Rodríguez).

0955-2219/$ – see front matter © 2007 Elsevier Ltd. All rights reserved.
doi:10.1016/j.jeurceramsoc.2007.02.179

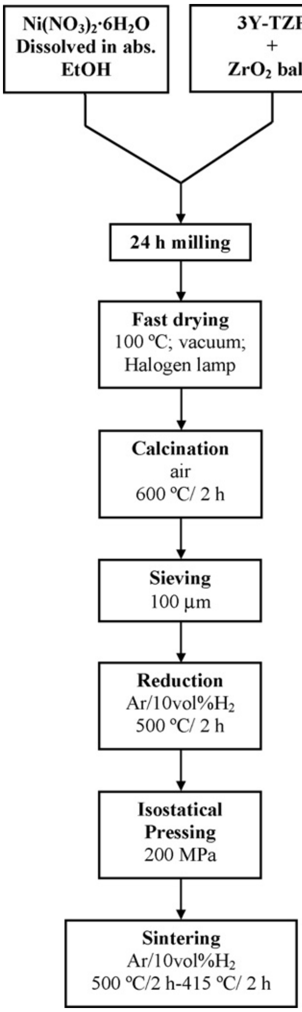

Fig. 1. Flow-chart of the experimental procedure followed to obtain dense nanocomposites.

Fig. 2. Device used for fast drying of the starting suspension with the help of an halogen lamp.

2.1.2. Nanopowder fabrication

Zirconia/nickel nanocomposites have been prepared by the deposition of nickel nanoparticles on the surface of the ceramic powders and fast drying in vacuum. A flow chart of the total powder processing can also be seen in Fig. 1. A previous detailed study was done to determine the most suitable salt for the deposition of Ni nanoparticles on the zirconia surface[6] and nickel nitrate hexahydrate was finally selected. The salt powders were weighed in order to fabricate the composites with different nickel content. The amount of salt corresponding to the metal volume fraction chosen had to be completely dissolved in a suitable volume of absolute ethanol with the help of ultrasonic agitation. When total nitrate dilution was achieved, 3YTZP powders were added and the suspension was milled for 24 h with zirconia balls. The mixture was dried drop by drop under vacuum at 100 °C and with the help of an halogen lamp, using the device showed in Fig. 2 and then calcined at 600 °C for 2 h in air to obtain ZrO_2/NiO mixed powders. Subsequently, the resulting powder was sieved down to 100 μm. Finally, the NiO was reduced to metallic nickel in a 90% Ar/10% H_2 atmosphere at 500 °C for 2 h. A TEM micrograph of the ZrO_2/Ni resulting powder is

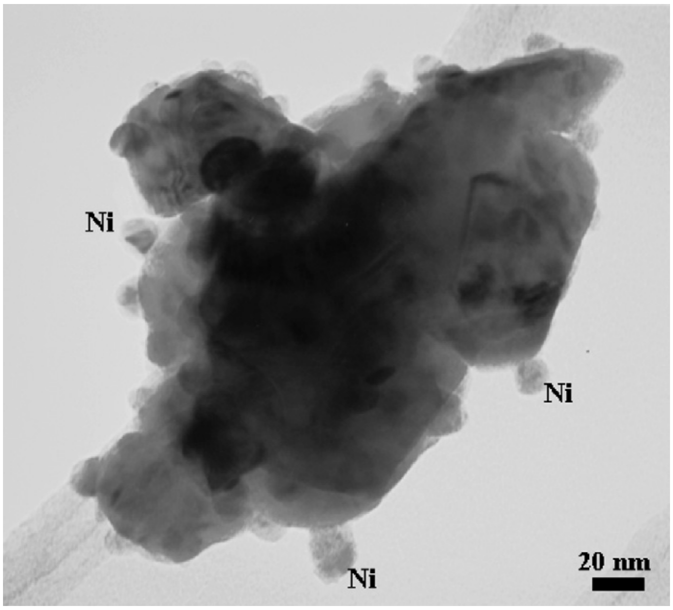

Fig. 3. TEM micrograph of a 3YTZP/2.5 vol.% Ni powder.

showed in Fig. 3. The study of the powders has revealed the absence of Ni particles larger than 50 nm.

2.1.3. *Pressing and sintering*

The powders were isostatically pressed at 200 MPa. The resulting bars, with approximated dimensions of 5 mm diameter and 50 mm long, were fired in a 90% Ar/10% H_2 atmosphere in two steps: (i) 500 °C for 2 h in order to reduce the NiO present in the surface of the starting Ni particles and (ii) at 1415 °C for 2 h for final sintering. The heating and cooling rate was kept at 600 °C/h.

2.2. *Microstructural characterization*

The microstructure of fired specimens was studied on surfaces polished down to 1 μm by optical microscopy and scanning electron microscopy (SEM, model DSM 960, Zeiss Thornwood, NY); in the case of deformed specimens, sections parallel to the compressive axis were cut from the samples. Thermal etching at 1250 °C for 30 min in 90% Ar/10% H_2 atmosphere was required to study the zirconia matrix grains. The Ni particle size distribution in the specimens was measured from transmission electron microscopy (TEM) images (JEOL microscope, model FXII, JEM 2000, operating at 200 kV) for powdered samples. For high-resolution transmission electron microscopy (HRTEM), a JEOL ARM microscope operating at 1250 keV was used for sintered samples.

A general overview of nickel and zirconia bonding and ZrO_2/Ni interfaces studied by HRTEM is showed in Fig. 4. A good interfacial bonding and low porosity in 3YTZP/n-Ni nanocomposites (referred hereafter to as n-Ni2.5, n-Ni5 and n-Ni10 according to vol.% of nickel content) have been observed from the microstructural characterization of dense samples.[7]

2.3. *Creep tests*

For creep tests, the specimens were cut in cylinders of 5 mm length and deformed in compression under constant load using a prototype creep machine described elsewhere.[10] These tests were carried out between 1200 and 1250 °C, to avoid grain growth, using nominal stresses, σ, between 32 and 66 MPa in argon atmosphere. Data were analyzed using the classical high-temperature creep equation[11]:

$$\dot{\varepsilon} = A\sigma^{n} \exp\left(\frac{Q}{RT}\right) \tag{1}$$

where $\dot{\varepsilon}$ is the strain rate deformation, A a constant including the grain size dependence, n the stress exponent, Q the activation energy, T the temperature and R is the gas constant. The creep parameters, n and Q, were determined from stress jumps under constant temperature conditions or temperature jumps under constant stress, respectively, performed during creep tests.

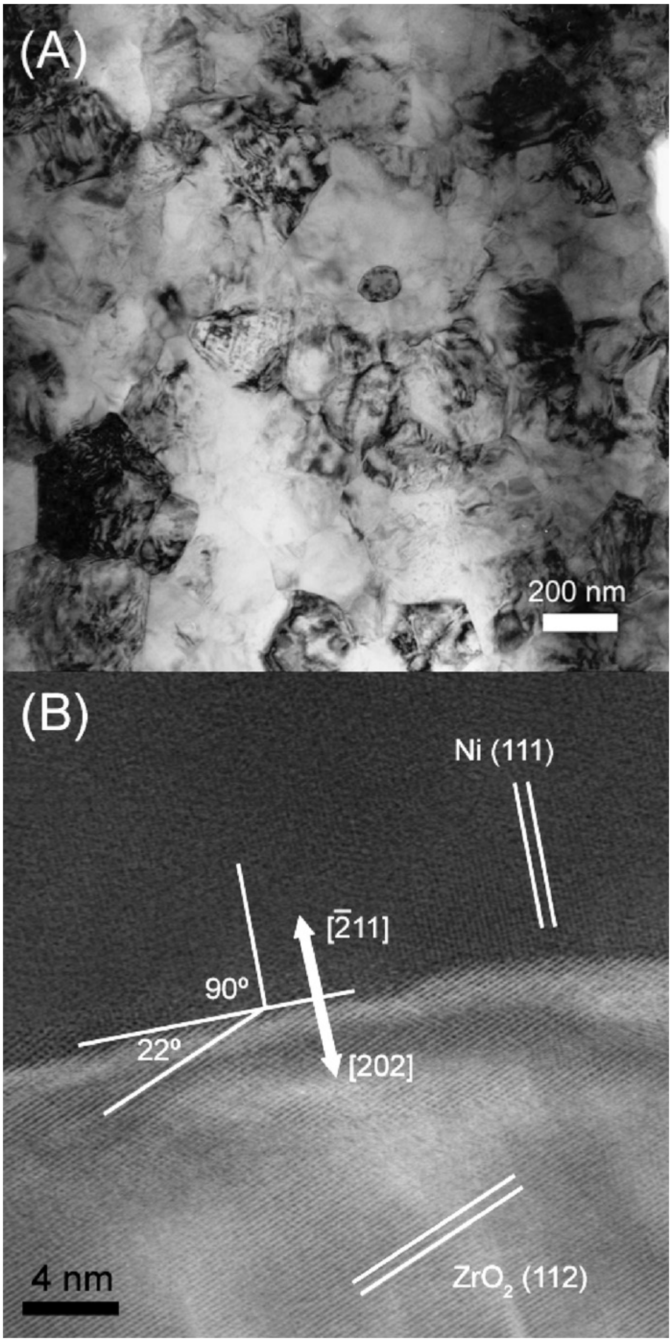

Fig. 4. (A) TEM micrograph of a general overview of nickel nanoparticles on zirconia surface in a sample with 10 vol.% Ni content. (B) Close up of a zirconia/Ni interface observed by HRTEM on the same sample.

3. Results and discussion

The as-received samples present nano- and submicrometric rounded nickel inclusions homogeneously distributed into equiaxed 3YTZP fine grains.[7] The average zirconia grain size is close to 200 nm for the three nanocomposites studied. Nevertheless, the nickel grain size increases with the amount of nickel; the average inclusion size is 60, 120 and 200 nm in n-Ni2.5, n-Ni5 and n-Ni10, respectively.

Fig. 5 shows a comparison of the creep curves for n-Ni5 and a μ-Ni composite[5] deformed at similar levels of stress and temperature. All nanocomposites have deformed at similar strain rates than n-Ni5, being more resistant than microcomposites by a factor close to 10. This discrepancy is easily explained in terms

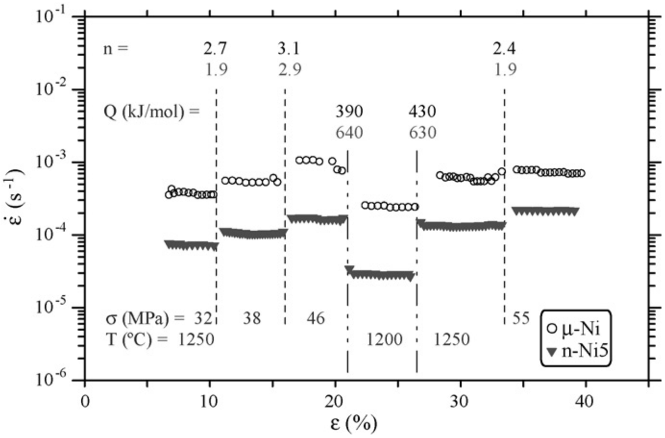

Fig. 5. Creep curves of μ-Ni[5] and n-Ni5 cermets deformed at similar levels of stress and temperature. The upper (lower) values of *n* and *Q* correspond to μ-Ni (n-Ni5).

of the different porosity levels between both materials[7]; after porosity correction of the μ-Ni creep curve,[5] the 3YTZP/μ-Ni creep rates are similar to those of 3YTZP/n-Ni cermets. The stress exponent values are similar to *n* obtained for μ-Ni, but higher values of *Q* have been measured for nanocomposites. Table 1 displays the creep parameters measured for the different 3YTZP/n-Ni composites; whereas the stress exponents of all nanocermets are similar, a tendency is observed in *Q* decreasing values with higher nickel contents. This influence of the amount of Ni content on *Q* values has not been measured in μ-Ni cermets,[5] where all studied compositions display a similar creep behavior at least up to 40 vol.% of Ni amount.

No microstructural changes have been observed after deformation. Either zirconia matrix or nickel inclusions do not undergo significant changes, showing the same values of grain size and shape than in as-received condition.

The absence of microstructural evolution during creep and *n* values obtained from creep tests suggest that n-Ni cermets deform by grain boundary sliding (GBS) of the 3YTZP grains with the concurrence of a threshold stress as in μ-Ni composites.[5] The existence of a threshold stress has been confirmed by $\dot{\varepsilon}$ versus $(\sigma-\sigma_0)^2$ plots of our experimental data accepting that the ceramic phase controls the creep properties.[4,5] Therefore, the creep rate of 3YTZP/n-Ni composites is correctly described by the following constitutive equation instead of equation (1):

$$\dot{\varepsilon} = A(\sigma-\sigma_0)^2 \exp\left(\frac{-Q}{RT}\right), \tag{2}$$

Table 1
Stress exponents and activation energies determined for 3YTZP/n-Ni composites using equation (1)

Sample	*n*	*Q* (kJ mol^{-1})
n-Ni2.5	2.6 ± 0.2	630 ± 80
n-Ni5	2.3 ± 0.4	590 ± 50
n-Ni10	2.2 ± 0.2	530 ± 50

Tests were performed under similar solicitation conditions in an argon atmosphere.

where σ_0 is similar to the threshold stress reported in high-purity YTZP polycrystals of the same average grain size[12] and also in 3YTZP/μ-Ni cermets.[5] Yttrium segregation towards grain boundaries, making GBS difficult, has been pointed out at the origin of the threshold stress.[12,13]

The previous analysis means that the creep parameters presented in Table 1 are apparent values. Although the stress exponent values drop to 2 taking into account the concurrence of σ_0, the *Q* values are still higher than reported for the activation energy in pure 3YTZP[12] and μ-Ni composites.[5] Furthermore, the tendency observed in *Q* (decreasing values with higher nickel contents) is not explained by the existence of a threshold stress; creep tests performed in similar stress and temperature conditions were expected to lead to similar apparent *Q* values, whereas our results show a clear dependence with nickel content.

Recently, the interfacial stability exhibited by nickel grains similar in size to 3YTZP one's (about 150–200 nm)[7] has been explained in terms of the existence of a small nickel oxide layer at the metal–ceramic interface.[14] The presence of these rich Ni–O bonding interfaces is likely to affect the activation energies for creep because of the influence on the path of the Zr diffusion that controls the accommodation mechanism in 3YTZP GBS. The model presented in Ref. 14 supposes that zirconium atoms diffuses along such Ni–O interfaces for 3YTZP in contact with Ni grains, where Zr migration is hindered by the strong Ni–O bonding energy. Then two types of 3YTZP grains can be identified in nanocomposites: (i) one group that are not in contact with nickel grains; this fraction of grains "A" slides each other as monolithic 3YTZP with an activation energy for creep corresponding to lattice cation diffusion and (ii) another proportion "B" of 3YTZP grains sharing at least one well-bonded interface with the nickel inclusions. In those well-matched grains, cations must diffuse along the ceramic–metal interface. The zirconium diffusion along those Ni–O boundaries could be responsible of the accommodation mechanism for creep in these nano-Ni composites resulting in higher values of *Q* as reported.[14]

In the light of this model, the *Q*-tendency observed in this study could be related to the proportion of well-matched metal–ceramic interfaces in the different nanocomposites better than to the nickel content itself. This proportion depends on the volume content and size of both 3YTZP and Ni phases. Microstructural analysis are now in progress to confirm this point.

4. Conclusions

Fast drying of nickel salts on zirconia powders is a capable technique to prepare nanopowder precursors leading to strong interfacial matching and low porosity in 3YTZP/n-Ni cermets. This work reports that the strong interface matching can be at the origin of the high activation energies for creep and these effective activation energies are sensitive to the amount of strongly-bonded TZP/Ni interfaces.

Acknowledgements

This work has been supported by the Spanish Ministry of Education and Science through the coordinated project

MAT2003-04199-CO2. S. Lopez-Esteban has been supported by the Spanish Ministry of Education and Science under Ramón y Cajal contract.

References

1. Reschke, S. and Bodganow, C., Engineering ceramics: new perspectives through value-added (multi-) functionality. *Key Eng. Mater.*, 1999, **175–176**, 1–10.
2. Qin, C.-D. and Derby, B., Diffusion bonding of nickel and zirconia: mechanical properties and interfacial microstructures. *J. Mater. Res.*, 1992, **7**, 1480–1488.
3. López-Esteban, S., Bartolomé, J. F., Moya, J. S. and Tanimoto, T., Mechanical performance of 3Y-TZP/Ni composites: tensile, bending, and uniaxial fatigue tests. *J. Mater. Res.*, 2002, **17**, 1592–1600.
4. Morales-Rodríguez, A., Bravo-León, A., Domínguez-Rodríguez, A. and Jiménez-Melendo, M., Creep of zirconia/nickel composites. *Mater. Sci. Forum*, 2004, **447–448**, 347–352.
5. Morales-Rodríguez, A., Microestructura y propiedades mecánicas a alta temperatura de compuestos circona-níquel. PhD thesis, Universidad de Sevilla, Sevilla, Spain, 2004.
6. Esteban-Betegon, F., Lopez-Esteban, S., Requena, J., Pecharroman, C., Moya, J. S. and Conesa, J. C., Obtaining Ni nanoparticles on 3Y-TZP powder from nickel salts. *J. Am. Ceram. Soc.*, 2006, **89**, 144.
7. Pecharromán, C., Beltran, J. I., Esteban-Betegon, F., Lopez-Esteban, S., Bartolome, J. F., Munoz, M. C. *et al.*, Zirconia/nickel interfaces in micro- and nanocomposites. *Zeit. Metall.*, 2005, **96**, 507.
8. Lopez-Esteban, S., Rodriguez-Suarez, T., Esteban-Betegón, F., Pecharromán, C. and Moya, J. S., Mechanical properties and interfaces of zirconia/nickel in micro- and nanocomposites. *J. Mater. Sci.*, 2006, **41**, 5194–5199.
9. Pecharroman, C., Esteban-Betegon, F., Bartolome, J. F., Richter, G. and Moya, J. S., Theoretical model of hardening in zirconia-nickel nanoparticle composites. *Nanoletters*, 2004, **4**, 747.
10. Gervais, H., Pellicier, B. and Castaing, J., Machine de fluage pour essais en compression à hautes températures de matériaux céramiques. *Rev. Int. Htes. Temp. et Réfract.*, 1978, **15**, 43–47.
11. Poirier, J. P., *Creep of Crystals*. Cambridge University Press, Cambridge, 1985, pp. 76–78.
12. Jiménez-Melendo, M., Domínguez-Rodríguez, A. and Bravo-León, A., Superplastic flow in fine-grained yttria-stabilised zirconium polycrystals: constitutive equation and deformation mechanism. *J. Am. Ceram. Soc.*, 1998, **81**, 2761–2776.
13. Domínguez-Rodríguez, A., Gómez-García, D., Lorenzo-Martín, C. and Muñoz-Bernabé, A., Influence of the yttrium segregation at grain boundaries in the superplasticity of yttria tetragonal zirconia polycrystals. *J. Eur. Ceram. Soc.*, 2003, **23**, 2969–2973.
14. Morales-Rodríguez, A., Gómez-García, D., García-Gañán, C., Solvas-Zapata, E. and Domínguez-Rodríguez, A., The role of metal ceramic interfaces on the high temperature mechanical response of nickel-yttria tetragonal zirconia polycrystals (Ni-YTZP). *J. Mater. Res.*, 2006, **41**, 5190–5193.